Fig.7

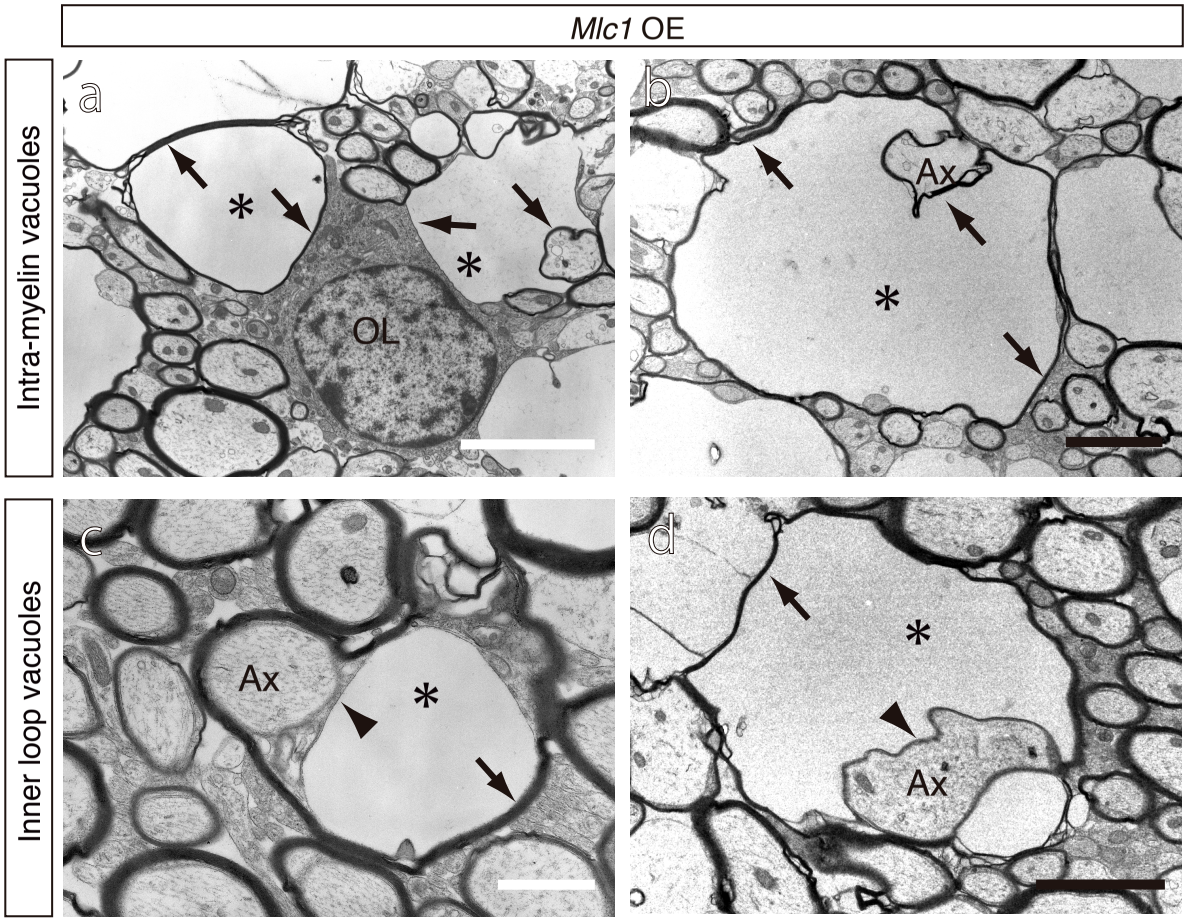
Intra-myelin vacuoles
Inner loop vacuoles
Mlc1 OE
a
b
c
d
OL
Ax
Ax
Ax
*
*
*
*
*

Fig. 7

High magnification views of oligodendrocyte associated vacuoles (asterisks in a-d). Typical features of intra-myelin vacuole: there were surrounded by myelin sheath as shown by electron-dense line (arrows in a, b). These vacuoles sometimes contained axon tracts that are also surrounded by the electron-dense line. Typical features of inner loop vacuole: the integrity of compact myelin was retained and vacuole were present between compact myelin and inner loop. Arrowheads in Fig.c and d indicate inner loop membrane. Arrows in Fig.c and d indicate myelin sheath. As: astrocyte, Ax: axon, BV: bood vessel, OL: oligodendrocyte, Black bar: 2μm, White Bar: 5μm

Fig.8

A

Mlc1-tTA:: Mlc1$^{tetO/tetO}$ bigenic mouse

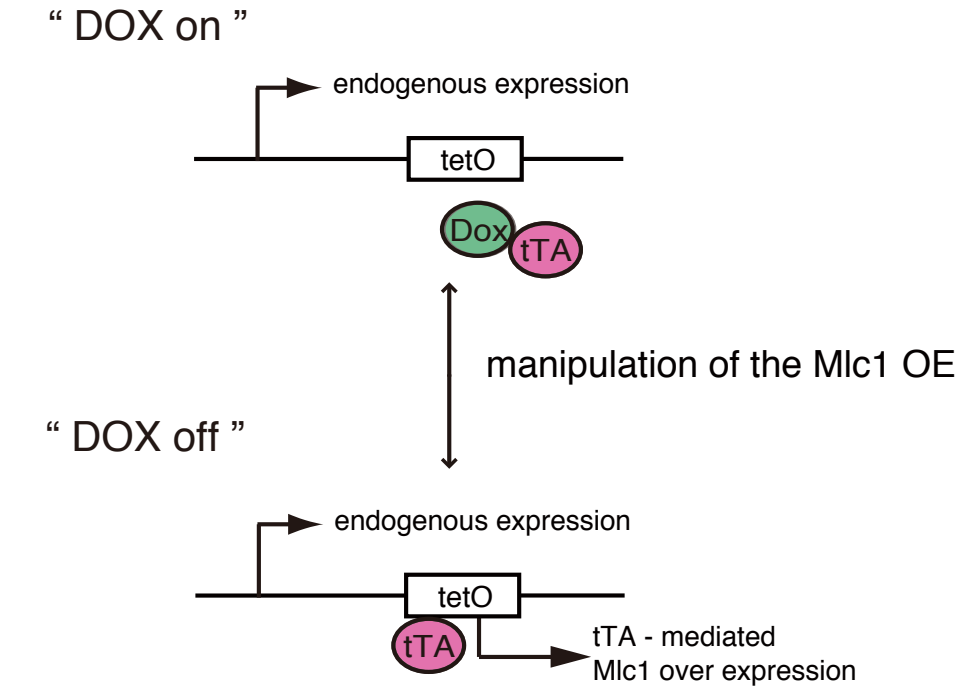

B

Mlc1 OE (P28-P38)

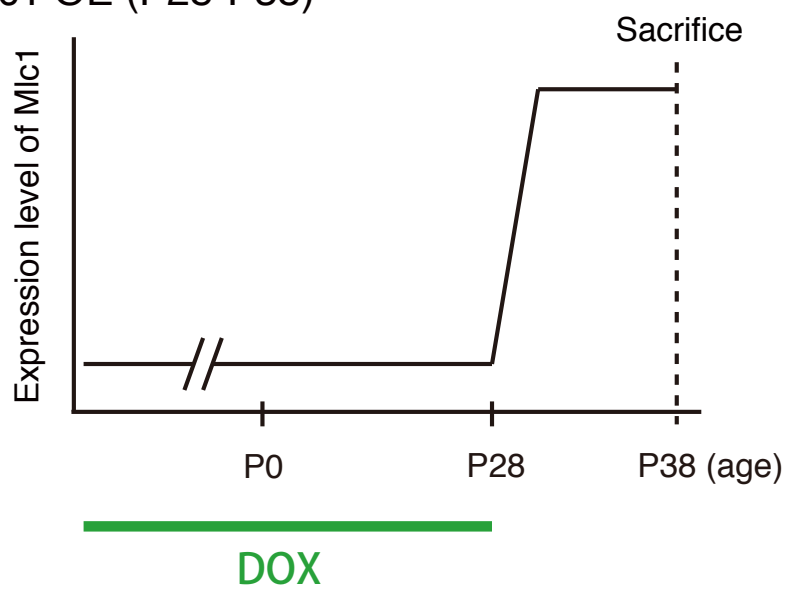

Fig.8

Schematic drawings showing manipulation of tTA-mediated Mlc1 overexpression.

(A) tTA-mediated Mlc1 overexpression was induced in a doxycycline (DOX) dependent manner. In the presence of DOX, tTA-mediated Mlc1 overexpression was cancelled and returned to the wild type expression (DOX on). In the absence of DOX, tTA-mediated Mlc1 overexpression was occurred (DOX off).

(B) Mlc1 overexpressing mouse fed with doxycycline-containing chows till postnatal days 28 (control) and then fed with normal chows for additional 10 days, resulting in the tTA-mediated Mlc1 overexpression only from postnatal days 28 to 38(Mlc1 $OE^{P28-P38}$).

Fig.9

A

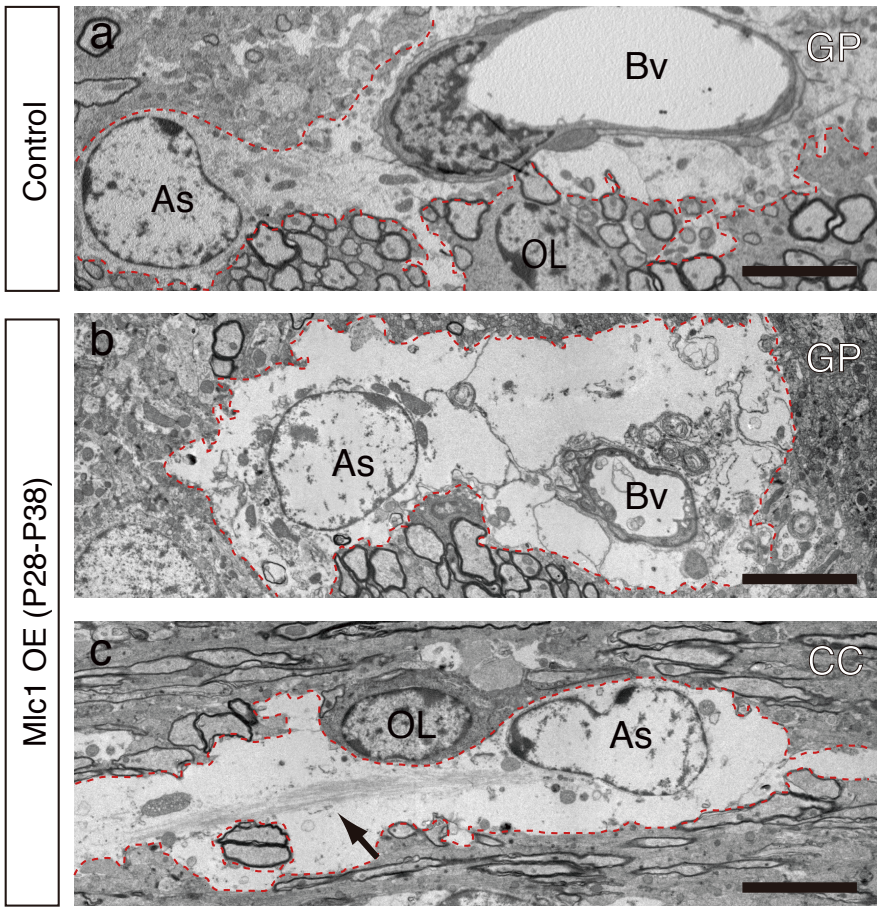
Control
a
Bv
GP
As
OL
Mlc1 OE (P28-P38)
b
GP
As
Bv
c
CC
OL
As

B

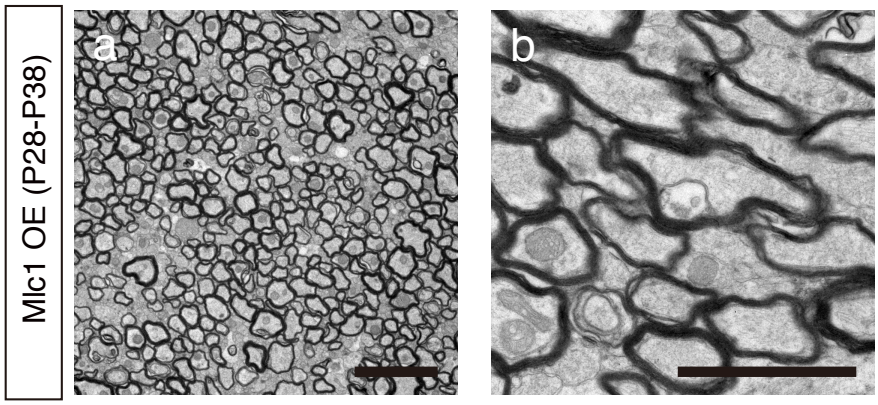
Mlc1 OE (P28-P38)
a
b

Fig.9

EM images of astrocyte in Mlc1 $OE^{P28-P38}$ and control mouse. No structural abnormalities were obvseved in the control (A-a). In Mlc1 $OE^{P28-P38}$, astrocytes surrounding blood vessel had more electron-lucent cytoplasm relevant to Mlc1 OE (A-b, c). Astrocyte was identified by the presence of intermediate filaments (arrow in A-c). Doted lines indicate periphery of astrocytes. Remarkably, myelin-associated vacuoles were not observed either low or high magnification views of EM images (B). As: astrocyte, Bv: blood vessel, OL: oligodendrocyte. Bar: 5μm.

Fig.10

A. OE (Whole)

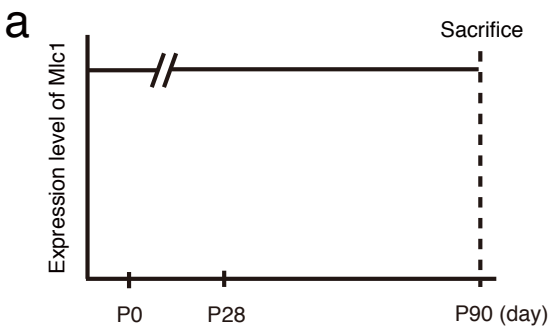

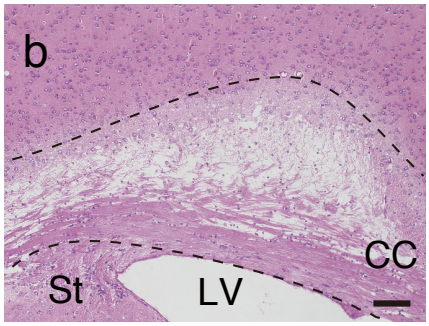

B. OE(embryo-P28)

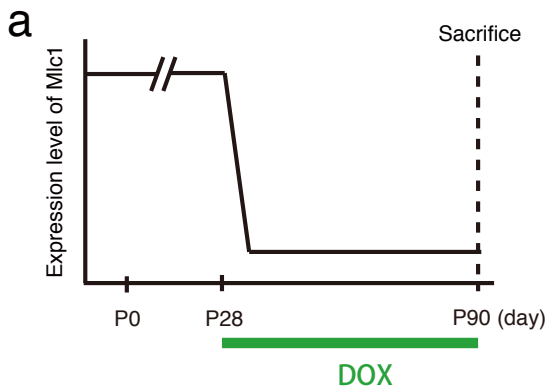

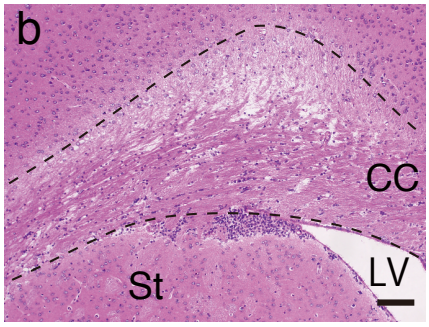

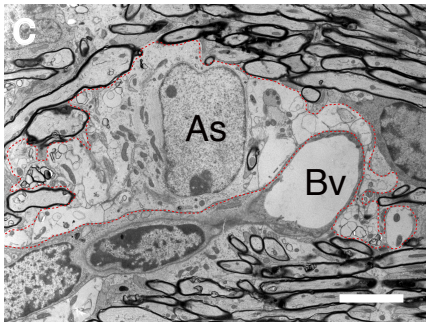

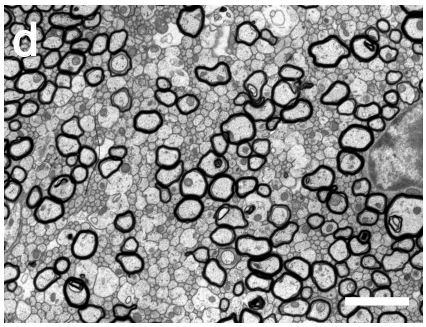

C.

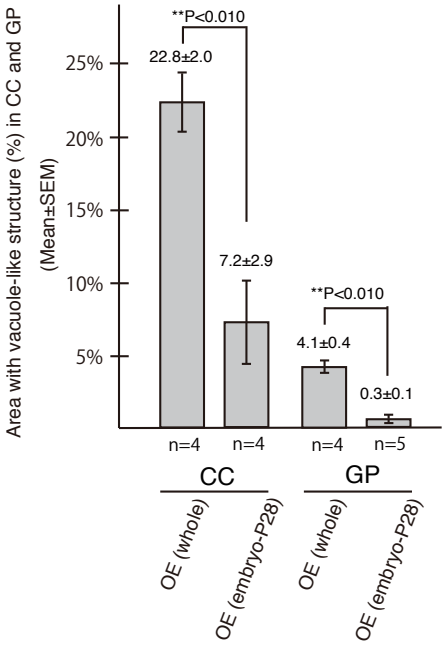

Fig. 10

(A) Mlc1 overexpressing mouse without DOX-feeding (A-a: OE^{whole}) had massive white matter vacuoles at postnatal days 90 (A-b).

(B) Mlc1 gene was overexpressed till the first month of age, which was by DOX-feeding until postnatal day 90 (B-a: $OE^{embryo\text{-}P28}$). In $OE^{embryo\text{-}P28}$ mouse, area with vacuole-like structure in white matter dramatically reduced after the cancellation of Mlc1 overexpression (B-b). Electron-lucent area occupied by swollen astrocytes were decreased (B-c). Myelin-associating vacuoles were not observed (B-d). As: astrocyte, Bv: blood vessel, CC: corpus callosum, Lv: lateral ventricle.

(C) Statistical analysis of the area with vacuole-like structure in LM study. Area with vacuole-like structure in CC and GP is shown (n=4 at least each points).

CC; corpus callosum, GP; globus pallidus. Black bar: 100μm, white bar: 5μm.

Fig.11

A. OE (DOX)

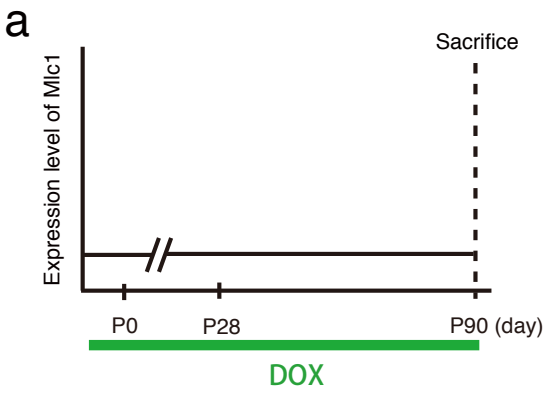

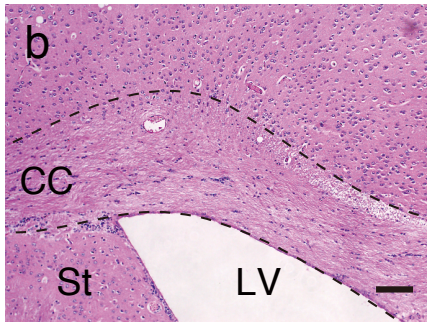

B. OE (P28-P90)

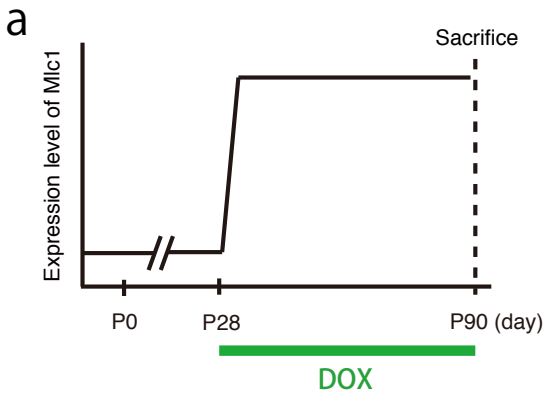

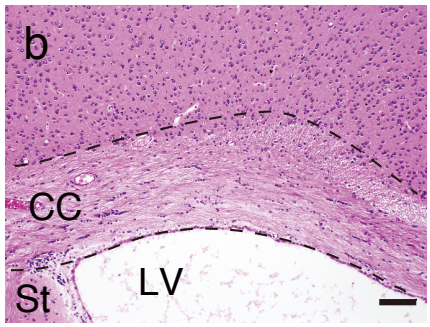

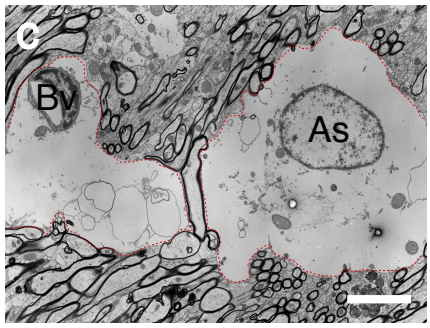

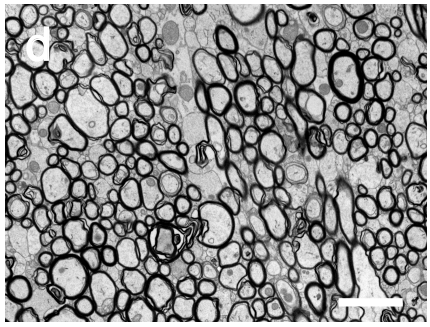

C

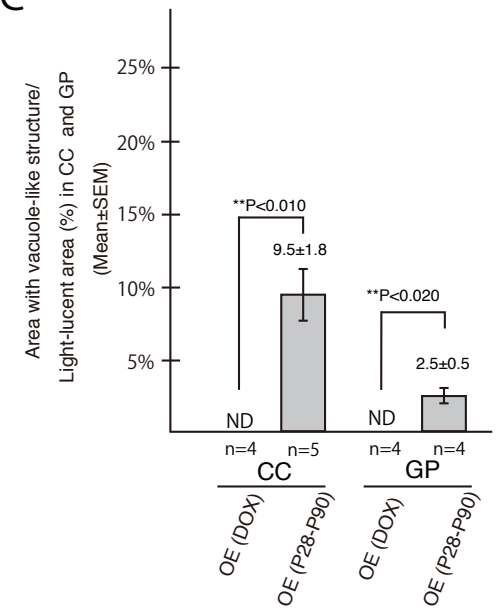

Fig. 11

Mlc1 overexpression induced after one month of age resulted in astrocyte swelling but no myelin vacuoles.

(A) Mlc1 OE mouse constantly fed with Dox (A-a: OE^{DOX}), no white matter abnormalities were observed by light miocroscopy (A-b).

(B) When Mlc1 was overexpressed after P28 by removing DOX from the food (B-a: $OE^{P28\text{-}P90}$), light-lucent area was statistically increased at P90, but no obvious vacuole-like structures were observed under light microscopy (B-b). EM images of $OE^{P28\text{-}P90}$. Astrocytes had electron-lucent and expanded cytoplasm relevant to OE^{whole} (B-c). No remarkable myelin-associating vacuoles were observed (B-d).
As: astrocyte, Bv: blood vessel, CC: corpus callosum, Lv: lateral ventricle. Black bar; 100 μm, White bar; 5 μm

C) Statistical analysis of the light-lucent area in LM study. Light-lucent area in CC and GP is shown (n=4 at least each points). CC; corpus callosum, GP; globus pallidus

Fig.12

A

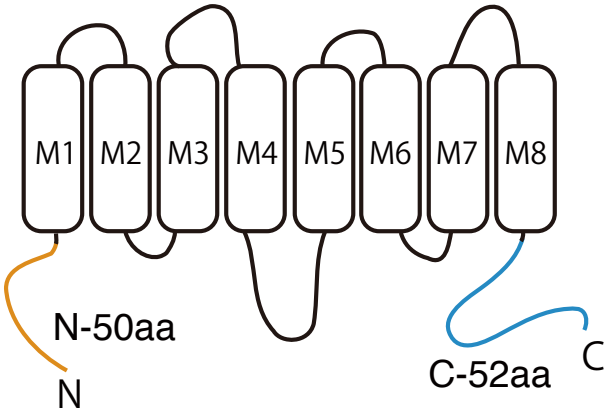
M1
M2
M3
M4
M5
M6
M7
M8
N-50aa
N
C-52aa
C

B

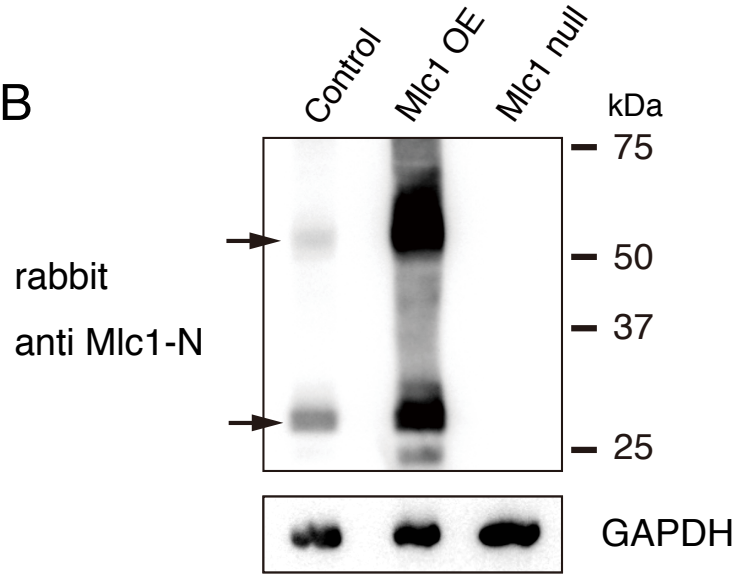
Control
Mlc1 OE
Mlc1 null
kDa
75
50
37
25
rabbit
anti Mlc1-N
GAPDH

C

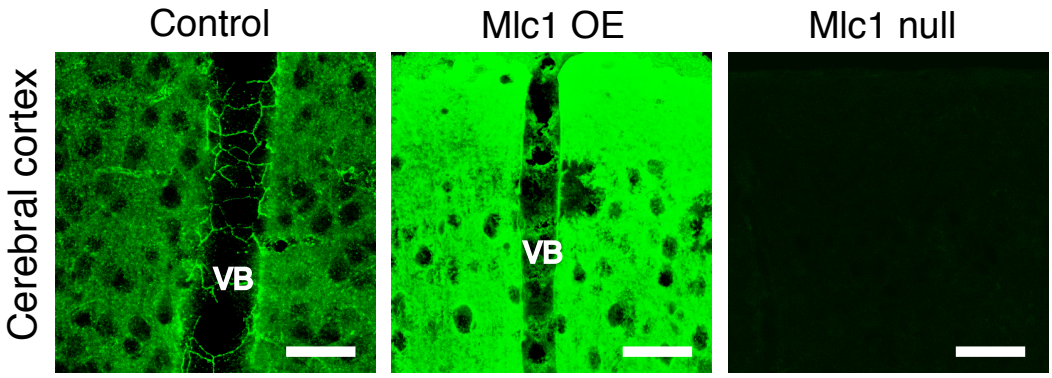
Control
Mlc1 OE
Mlc1 null
Cerebral cortex
VB
VB

Fig. 12

Development of new primary antibodies recognizing mouse MLC1

(A) Schematic drawing of epitopes used for development of anti MLC1 antibodies. Antibodies against 50 amino acids (aa) of N-terminal or 52 aa of C-terminal were risen in rabbit and guinea pig.

(B) Western blotting for newly developed Mlc1 antibody. Rabbit derived anti Mlc1-N antibody was used. Newly developed antibody was able to recognize both monomer (30kDa) and dimmer forms (60-70kDa) of Mlc1. No bands were detected in Mlc1 null specimen (arrows in B), while strong bands were observed in Mlc1 overexpressing

(C) Immunohistochemistry for developed Mlc1 antibody. Rabbit derived anti Mlc1-N antibody was used. Mlc1 immunoreactivity was detectable only in astrocyte lineage cells. Punctate immunoreactivity was scattered and concentrated at the surfaces contacting the blood vessel in the control specimen (Fig. C). No immunoreactivity was detected in Mlc1 null specimens (B, C), while strong immunoreactivity were observed in Mlc1 overexpressing specimens (B, C). VB; blood vessel, Scale bar: 50 μ m.

Fig.13

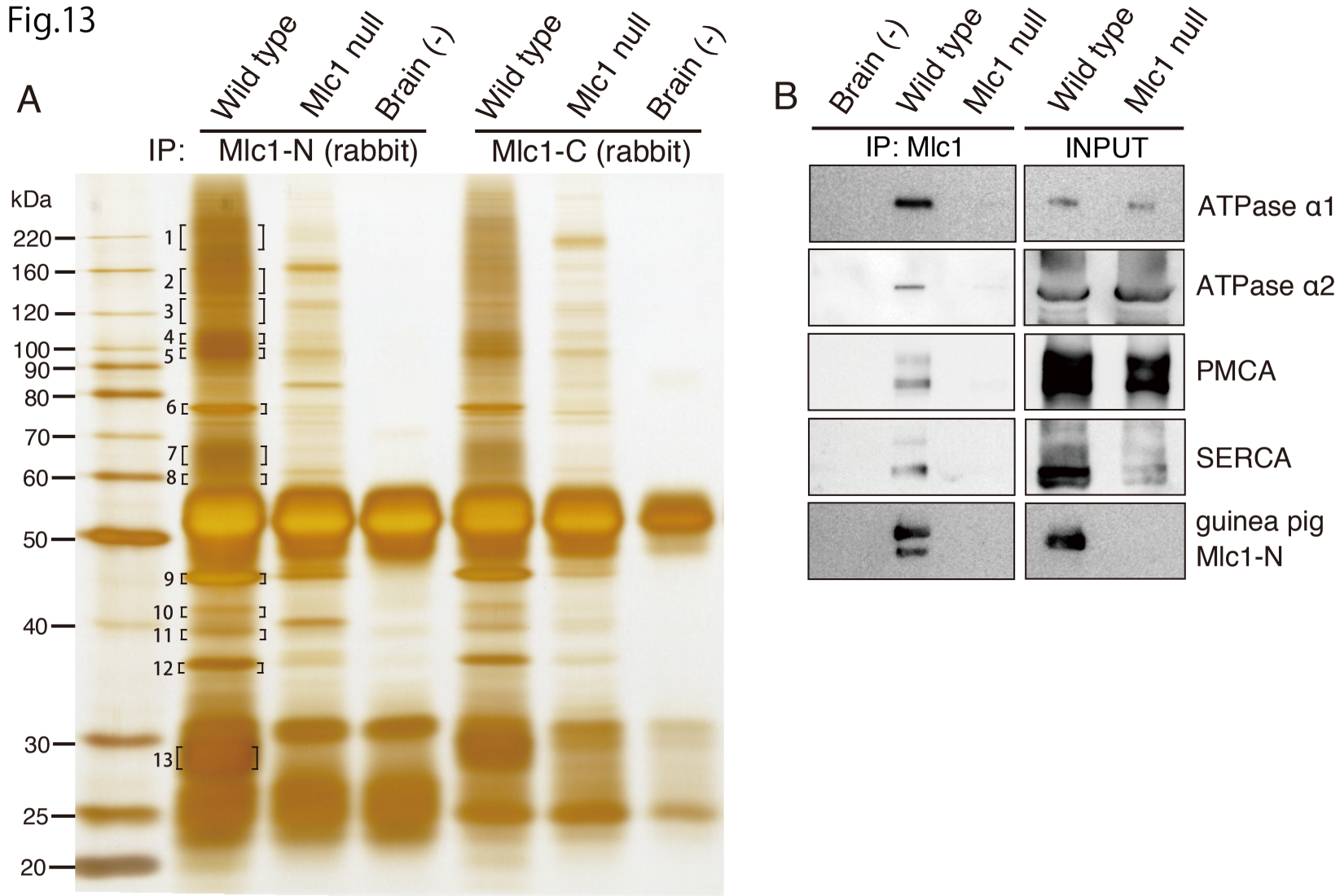
A
Wild type
Mlc1 null
Brain (-)
Wild type
Mlc1 null
Brain (-)
IP:
Mlc1-N (rabbit)
Mlc1-C (rabbit)
kDa
220
160
120
100
90
80
70
60
50
40
30
25
20
1
2
3
4
5
6
7
8
9
10
11
12
13
B
Brain (-)
Wild type
Mlc1 null
Wild type
Mlc1 null
IP: Mlc1
INPUT
ATPase α1
ATPase α2
PMCA
SERCA
guinea pig
Mlc1-N

Fig. 13

Membrane extract was prepared from the wild type and Mlc1 null mice, then immunoprecipitated with ether rabbit Mlc1-N or rabbit Mlc1-C antibody. Immunopresipitation from samples with no brain extract was used as a negative control (Brain minus in A and B).

(A)Each precipitates were separated by SDS-PAGE and silver stained. Intensely stained bands were detected in the wild-type immonoprecipitate (parentheses in A) and less so in Mlc1-null and the no brain control. Reproducible stained patterns were obtained from immunprecipitates with rabbit Mlc1-N and with Mlc1-C antibody. Intensely stained bands in the wild type were dissected and proceeded to mass spectrometry analysis. The result of mass spectrometry was represented in Table 1.

(B) Western blotting for candidate proteins. P-type ATPase members (Na^+/K^+ ATPase α1, Na^+/K^+ ATPase α2, PMCA, and SERCA) were detected in the wild type immunoprecipitate and it is nearly undetectable both in Mlc1 null immunoprecipitate and no brain control. Mlc1 is also detected in wild type immunoprecipitate by using guinea pig Mlc1-N antibody.

Fig.14

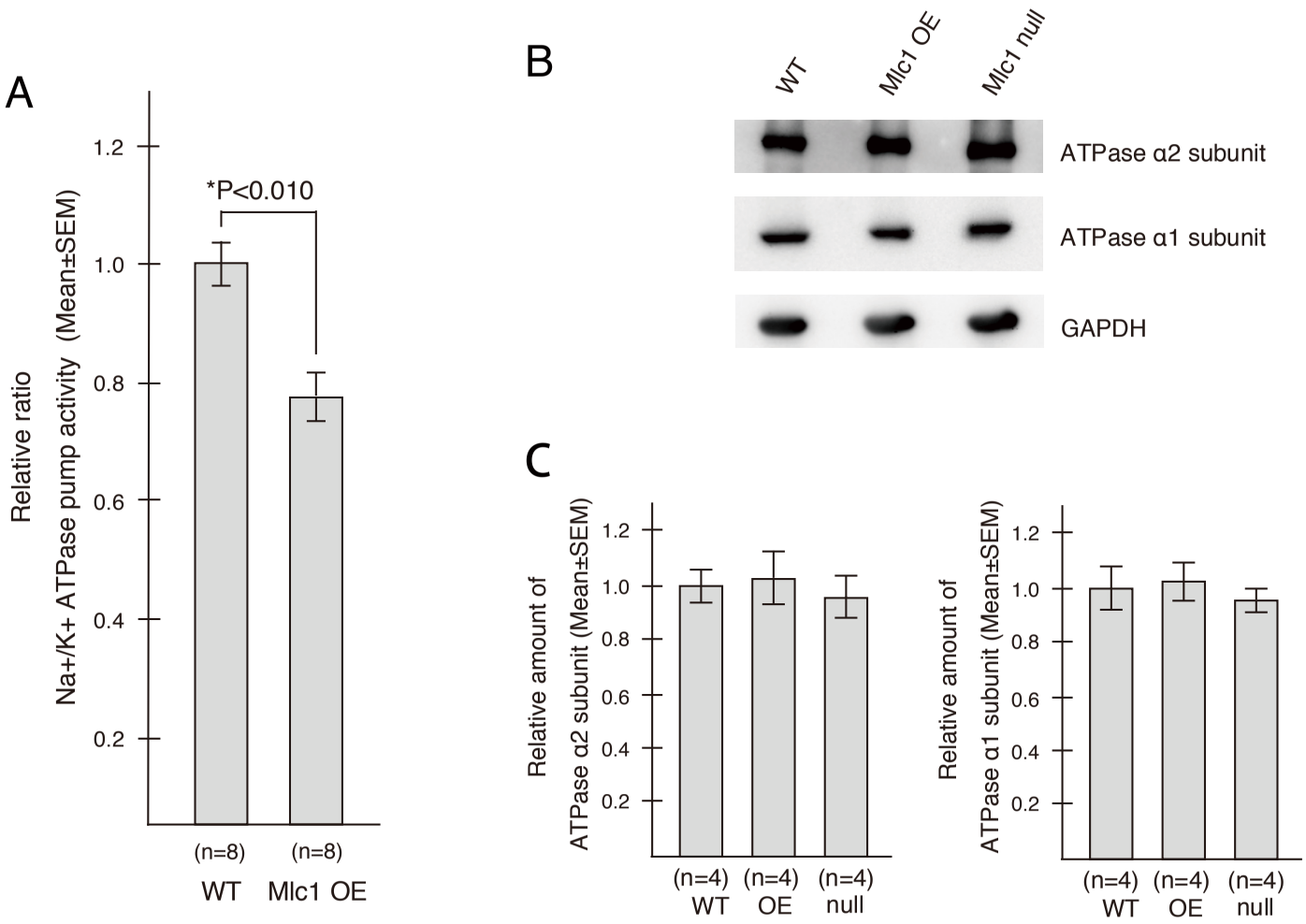
A
Relative ratio
Na+/K+ ATPase pump activity (Mean±SEM)
1.2
1.0
0.8
0.6
0.4
0.2
*P<0.010
(n=8)
(n=8)
WT
Mlc1 OE
B
WT
Mlc1 OE
Mlc1 null
ATPase α2 subunit
ATPase α1 subunit
GAPDH
C
Relative amount of
ATPase α2 subunit (Mean±SEM)
1.2
1.0
0.8
0.6
0.4
0.2
(n=4)
(n=4)
(n=4)
WT
OE
null
Relative amount of
ATPase α1 subunit (Mean±SEM)
1.2
1.0
0.8
0.6
0.4
0.2
(n=4)
(n=4)
(n=4)
WT
OE
null

Fig. 14

Sodium pump activity is reduced in Mlc1 OE astrocytes.

(A) Rubidium-86 (^{86}Rb) uptake assay. Sodium pump activity was statistically reduced by 77% control level ($P<0.010$). Vertical axis indicates the relative ratio against those of wild type and represented Mean±SEM (n=8).

(B) Semi-quantitative analysis for Na^+/K^+ ATPase α2 and α1 subunit. Membrane extract from wild type, Mlc1 OE, and Mlc1 null mouse were separated by SDS-PAGE and western blotting was performed. Band intensity was normalized against GAPDH, and the each protein level was semi-quantitatively analyzed.

(C) No significant differences in the protein expression level of α subunits among Mlc1 null, wild type and Mlc1 OE mice were detected ($P>0.050$, n=4).

Fig.15

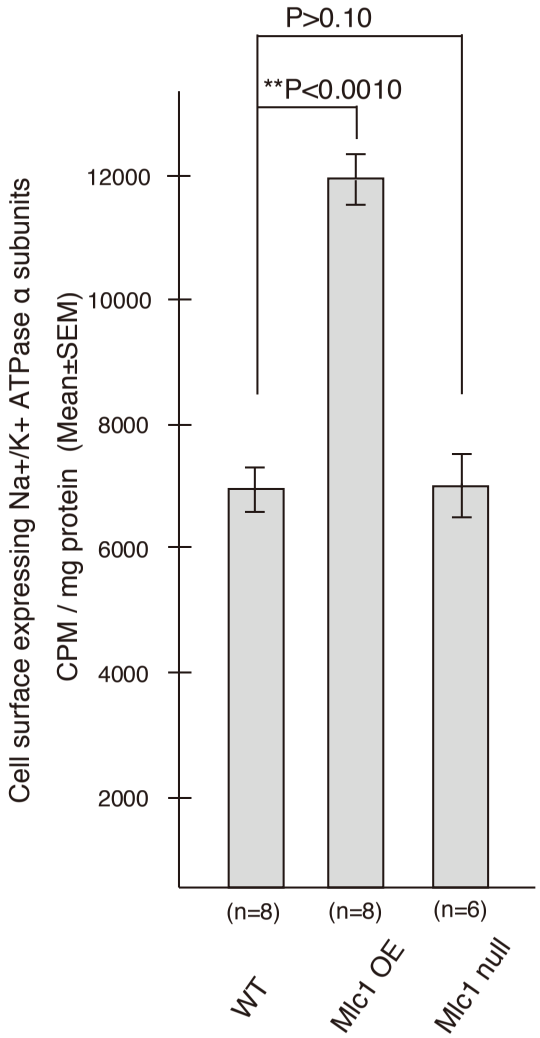
A
P>0.10
**P<0.0010
Cell surface expressing Na+/K+ ATPase α subunits
CPM / mg protein (Mean±SEM)
12000
10000
8000
6000
4000
2000
(n=8)
(n=8)
(n=6)
WT
Mlc1 OE
Mlc1 null

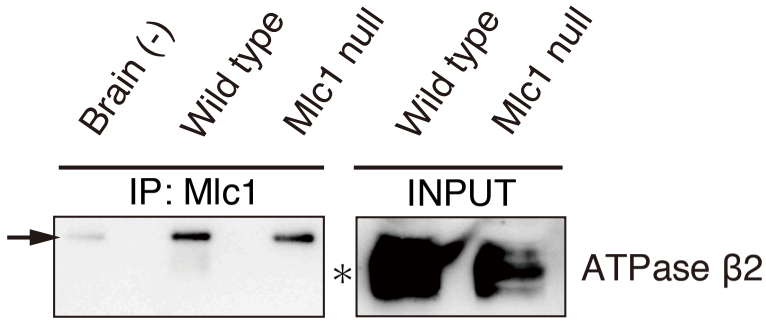
B
Brain (-)
Wild type
Mlc1 null
Wild type
Mlc1 null
IP: Mlc1
INPUT
*
ATPase β2

Fig. 15

(A) ^{3}H-ouabain binding assay. Cell-surface expressing Na^{+}/K^{+} ATPase α subunits were dramatically increased in Mlc1 OE astrocyte ($P<0.0010$), whereas no significant differences between Mlc1 null and wild type mice were detected ($P>0.10$). Radioactivity that bound cell surface expressing Na^{+}/K^{+} ATPase α subunits represented by CPM/mg protein (Mean±SEM, n=6 at least each points).

(B) Na^{+}/K^{+} ATPase β 2 subunit did not interact with Mlc1. The same sets of immunoprecipitates with Fig.13B were separated by SDS-PAGE and western blotting for Na^{+}/K^{+} ATPase β 2 subunit was performed. No clear band for Na^{+}/K^{+} ATPase β 2 subunit was detected in the wild type. Arrow indicates the band of IgG. Asterisk indicates band of Na^{+}/K^{+} ATPase β 2 subunit.